*J. Chem. Sci.* (2020) 132:110
https://doi.org/10.1007/s12039-020-01819-9


REGULAR ARTICLE

# High throughput green reduction of tris(p-nitrophenyl)amine at ambient temperature over homogenous AgNPs as H-transfer catalyst

SAEED REZA HORMOZI JANGI* and MORTEZA AKHOND
Massoumi Laboratory, Department of Chemistry, College of Sciences, Shiraz University, Shiraz 71454, Iran
E-mail: saeedrezahormozi@gmail.com; akhond@shirazu.ac.ir

MS received 31 May 2020; revised 30 June 2020; accepted 6 July 2020

**Abstract.** A green, facile, fast, and high throughput reusable catalytic reduction process was developed for the large-scale reduction of tris(p-nitrophenyl)amine to its corresponding amino-compound, tris(p-aminophenyl)amine (TAPA). The homogenous AgNPs and $NaBH_4$ were used as the H-transfer catalyst and the H-donor compound, respectively. The successful reduction of TNPA was investigated by FT–IR, EDX, and XRD analysis, and its optical properties were checked by the UV–Visible and FL spectroscopies. Factors affecting the reduction yield including, temperature, reaction time, mmol of $NaBH_4$, and catalyst volume, were optimized. Although the AgNPs are homogenous, both TNPA and TAPA are insoluble in water (AgNPs), hence the reduction process is heterogeneous. The importance of the heterogeneous reduction of TNPA was investigated, indicated that the reduction yield reached its maximum value when TNPA heterogeneously reduced on the surface of AgNPs. The reduction yield at optimal conditions was calculated at about 98.0% for the first and 72.0% after the 6$^{th}$ operational cycle, respectively. The mechanism of the reduction process was also established, indicated that the process works through a possible Langmuir–Hinshelwood mechanism. The easy recovery and excellent reusability of homogenous AgNPs along with high reaction yield reveal the power of the proposed method for the reduction of nitro-compounds.

**Keywords.** Green catalysis; Reduction of tris(p-nitrophenyl)amine; Tris(p-aminophenyl)amine (TAPA); Reusable catalyst.

## 1. Introduction

The efficient reduction of nitroaromatic compounds into their more-useful amino-compounds is one of the most attractive fields for recent researches because they are common organic pollutants in agricultural and industrial wastewaters.[1,2] The corresponding amino-products have several applications in synthetic chemistry.[3] The traditional methods for the hydrogenation of nitroaromatics employ some homogeneous classic metal catalysts. Generally, the reduction performs using hydrazine, hydrogen, or $NaBH_4$ as the H-donor and platinum or palladium as the catalyst.[1,3,4]

Recently, noble metal nanoparticles,[5,6] and their nanocomposites[1,7–12] have been employed for the reduction of nitroaromatics. In this regard, several high throughput nanocatalysts were synthesized and characterized for the reduction of nitro compounds, for instance, gold NPs, platinum NPs, palladium NPs, Ag/$TiO_2$,[1] AgNPs/porous silicon,[7] AuPd–$Fe_3O_4$ NPs,[9–11] and porous carbon materials restricted gold catalyst.[12] Moreover, graphitic carbon nitride nanocomposites (g-$C_3N_4$) have been utilized for the reduction of nitroaromatics.[13–16] The reduction process can occur through the chemical, electrochemical, or even photocatalytic mechanisms. Regarding these nanocatalysts, Rh/$Fe_3O_4$/g-$C_3N_4$gold,[14] g-$C_3N_4$@$Fe_3O_4$,[15] and Ni@g-$C_3N_4$ nanohybrids[16] were previously used for reduction purposes. Besides, Qin *et al.,* developed a highly efficient nanocatalyst by the *in-situ* deposition of gold nanoparticles onto polydopamine-decorated g-$C_3N_4$.[13] In addition, Rajesh and Venkatesan encapsulated AgNPs into graphite grafted with hyperbranched poly(amidoamine) dendrimer. They

*For correspondence

*Electronic supplementary material: The online version of this article (https://doi.org/10.1007/s12039-020-01819-9) contains supplementary material, which is available to authorized users.*

Published online: 18 August 2020

investigated the catalytic activity of this nanocatalyst towards the reduction of nitroaromatics.[8]

Usually, the nitroaromatics reduction performs in the presence of $NaBH_4$ as the H-donor compound.[1,3,5–9,17] However, hydrazine hydrate has also been used for the reduction of aromatic nitro compounds in the presence of the iron oxide/hydroxide or Pd/C as the H-transfer catalyst.[4] In 2018, a textile-supported silver nanoparticles catalyst was reported for the reduction of nitroaromatics in the presence of $NaBH_4$ as the H-donor and $THF/H_2O$ as the reaction solvent with a yield at the range of 33.50-91.2% and reaction time between 3-12 h for the different substrates.[3] Another, excellent record in this field is the development of a novel graphene oxide-supported palladium nanoparticles for the reduction of nitroaromatics, reported in 2019.[18]

In this study, a facile, fast, and high throughput reusable catalytic reduction process was developed for the large-scale reduction of tris(p-nitrophenyl)amine to its corresponding amino-compound, tris(p-aminophenyl)amine (TAPA). The homogenous AgNPs and $NaBH_4$ were used as the H-transfer catalyst and the H-donor compound, respectively. Factors affecting the yield of the TNPA reduction including, temperature, reaction time, mmol of $NaBH_4$, and catalyst volume, were optimized. As a significant advantage, the developed method works through a green chemistry approach. The successful reduction of TNPA was investigated by FT-IR, EDX, and XRD analysis, and its optical properties were checked by the UV-Visible and FL spectroscopies. Also, the importance of the heterogeneous reduction of TNPA, the mechanism of the reduction, and the reusability of the catalytic system were evaluated.

## 2. Experimental

### 2.1 *Synthesis of AgNPs*

Silver nanoparticles (AgNPs) were synthesized based on the literature.[19] Briefly, 5.0 mL of 10.0 mM $AgNO_3$ (Merck) was mixed with 5.0 mL sodium citrate (10.0 mM, Merck). After that, 89.0 mL DI water (Zolal Teb Shimico (Iran) company) was added to the mixture. Then, the resulting solution was incubated for 20 min at room temperature. The synthesis process was followed by the quick addition of $NaBH_4$ (8.8 mg, Merck) and stirring for 2.0 hours at ambient temperature. Finally, the yellow-coloured silver nanoparticles were stored under dark conditions (4 °C) for future uses. It should be mentioned that the mass concentration of the as-synthesized AgNPs was estimated at about 150 μg $mL^{-1}$.

### 2.2 *Synthesis of TNPA*

In a typical experiment, 2.54 mmol of 1-choloro-4-nitrobenzene (p-ChNB, Merck) was mixed with 1.27 mmol of 4-nitroaniline (4-NA, Merck). Then, 2.0 mL DMSO (Merck) was added to the above solid mixture. The synthesis process was followed by the quick addition of 1.77 mmol cesium iodide (Merck) and 1.33 mmol $K_2CO_3$ (Merck). After that, the resulting solution was refluxed at 140 °C for 17 h. After this time, the reaction mixture was changed to a blue viscose solution. This solution was cooled down to room temperature, and the TNPA was precipitated by the addition of the appropriate amount of DI water. The reaction mixture was then centrifuged, and the fine-yellow powder of TNPA was collected. The collected product was dissolved in the acetone and further precipitated by DI water and centrifuged. These steps were performed five times for obtaining the fine-pure product. The reaction yield was estimated at about 74.0%.

### 2.3 *Lab-scale and Large-scale reduction of TNPA*

TNPA was heterogeneously reduced by $NaBH_4$ on the surface of the homogenous AgNPs. Although the AgNPs are homogenous, both TNPA and TAPA are insoluble in water (AgNPs), so the reduction process is heterogeneous. At the optimal conditions, 0.20 mmol of TNPA powder was added to 4.5 mL of AgNPs, containing 1.0 mmol $NaBH_4$ as the H-donor compound. Then, the mixture was stirred at the ambient temperature for 3.0 hours. The workup of the resulting pale-grey-reddish-grey tris(p-aminophenyl)amine (TAPA) powder was performed by filtration and then by crystallization from acetone. After that, the TAPA was dried at 37 °C. The AgNPs (contained unreacted $NaBH_4$) were collected and directly used for the reusability studies. At the optimal conditions, the reaction yield was calculated at about 98.0%.

The TNPA reduction was also scaled up for investigating the power of the developed method for the large-scale synthesis of TAPA. To do this, 7.6 gr of TNPA powder was added to AgNPs solution (150.0 μg $mL^{-1}$), containing 3.8 gr $NaBH_4$ (with a final concentration of 200 mg $mL^{-1}$ in the reaction media). The mixture was stirred at ambient temperature for 3.0 hours, and then the resulting TAPA

powder (5.5 gr) was collected by filtration and then by crystallization from acetone.

### 2.4 *Instrumentation for material characterization*

An Ultrospec 4000 UV-Vis spectrophotometer manufactured by Pharmacia Biotech (Biochrom) Ltd. equipped with SWIFT Software and a Metrohm 827 pH lab pH meter equipped with a combined glass electrode were used. TEM micrographs were done by electron microscope (Zeiss, model EL10C) operated at an accelerating voltage of 80 kV. The FT-IR analysis was performed by a spectrum RX1 (Perkin Elmer, 940 Winter Street, Waltham, and Massachusetts 02451, USA). The XRD and EDX spectra were recorded by employing Rigaku D/max-3C (Japan, www.rigaku.com/en) with Cu-Kα (λ = 1.54 nm) radiation line and MIRA3-TESCAN (15 KV, www.tescan.com) electronic microscope, respectively. The fluorescence spectra were recorded using a Perkin-Elmer LS50B spectrofluorometer, equipped with a thermostated cell compartment and 1.0 cm quartz cuvettes.

## 3. Results and Discussion

### 3.1 *Characterization of AgNPs*

The optical properties of AgNPs and their size and morphology were characterized by UV–Visible spectroscopy and TEM imaging, respectively (Figure 1). The UV–Vis. spectrum of AgNPs exhibited a $\lambda_{max}$ at 390 nm for the as-synthesized AgNPs that is in good agreement with the previous reports in the literature,[19] indicating the successful synthesis of AgNPs. Regarding the TEM image of AgNPs, the AgNPs are uniform and have a size of about 12.0 nm.

### 3.2 *Characterization of TNPA*

The TNPA was characterized by FT–IR, XRD, EDX, UV–Visible, and FL spectroscopy. First, the FT-IR analysis was employed for the characterization of the as-synthesized TNPA. In this regard, the FT–IR spectra of the reactants (1-choloro-4-nitrobenzene and 4-nitroaniline) and the resulting TNPA were recorded (Figure S1, Supplementary Information). Based on these spectra, the FT–IR peaks at 533 and 740 $cm^{-1}$ are assigned to the C–Cl in 1-choloro-4-nitrobenzene. Besides, the IR bands at 1342 and 1535.7 $cm^{-1}$ are related to the $–NO_2$ group. Based on the spectrum b (4-nitroaniline), the absorption bands at 3361.78 and 3481 $cm^{-1}$ are attributed to the $–NH_2$ group. Moreover, the peaks at 1300 and 1473.7 $cm^{-1}$ are assigned to the $–NO_2$ group. Also, the peak at 1623.15 $cm^{-1}$ is related to the N–H bending of the primary amines. However, in the spectrum c (TNPA spectrum), the $–NH_2$ and C–Cl peaks of the reactants were not observed. Besides, the band at 1200 $cm^{-1}$ and 1651.38 $cm^{-1}$ in this spectrum are attributed to the –C–N and C=C groups, respectively. The absence of the N–H stretch (no peaks in 3340 and 3460 $cm^{-1}$) in this compound, exhibited that it is a tertiary amine. Additionally, the IR bands at 1535.13 and 1314.3 $cm^{-1}$ are attributed to the $–NO_2$ groups. It must be noted that the FT–IR spectrum of TNPA is consistent with the previously reported FT–IR spectrum for TNPA,[20] indicating the successful synthesis of TNPA. The EDX analysis was carried out to shine the FT–IR results (Figure S2a, Supplementary Information).

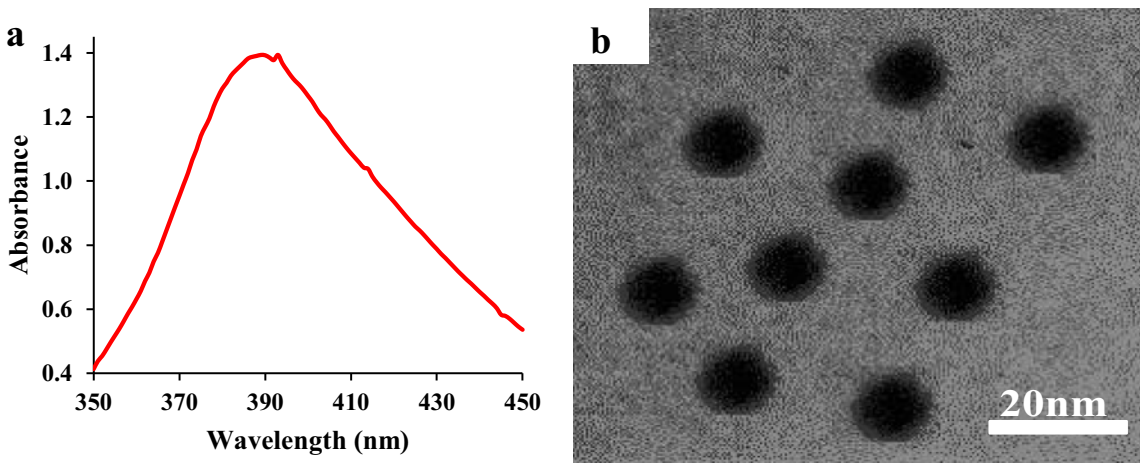


**Figure 1.** UV-Vis spectrum (a) and TEM image (b) of AgNPs.

Regarding Figure S2a, only the lines of O, N, and C were observed in the EDX spectrum of the TNPA. Hence, the EDX analysis attests to the FT-IR results.

The XRD spectrum of TNPA was recorded for the investigation of its crystalline structure (Figure S2b, Supplementary Information). The XRD peaks positioned at 2θ=13.3148, 14.5941, 16.8198, 18.6594, 19.1868, 24.006, 26.1815, 26.849, 27.5999, 28.3731, and 29.9472 can be assigned to C(200), C(210), C(211), C(222), C(300), C(320), C(400), C(333), C(410), and C(420), respectively. Based on the XRD pattern, the d-spacing and the average crystalline size of TNPA were estimated as 4.0 °A and 47.3 nm, respectively. The optical properties of the fine-yellow TNPA powder were checked by UV-Visible (Figure S3a, Supplementary Information) and FL spectroscopies (Figure S3b). Regarding the absorption spectrum, two characteristic absorption peaks at 237 nm and 400 nm were observed for the TNPA. The peak at 400 nm can be related to the triphenylamine part of TNPA, as reported.[21] The peak at 237 nm is attributed to the π–π* (aromatic ring structure).[19] Moreover, the aromatic ring showed a peak at 250 nm[21] that this peak was shifted to 237 nm in the TNPA spectrum due to the conjugation effects of the $–NO_2$ groups with π–electrons of the aromatic rings, as reported.[22] Regarding the fluorescence spectrum of TNPA, the excitation and emission wavelengths for TNPA were observed at 250 nm and 502 nm, respectively.

### 3.3 *Characterization of TAPA*

The as-synthesized TAPA was characterized using FT–IR, EDX, XRD, UV–Visible, and FL spectroscopy. It should be noted that the chemical structures of both TNPA and TAPA are shown in Figure S4 (Supplementary Information). Figure S5 (Supplementary Information) shows the FT–IR spectra of both TNPA and its reduction product (TAPA). Concerning this figure, the peaks at 1200 and 1651.38 $cm^{-1}$ in both spectra are related to the C–N[23] and C=C groups, respectively. The absence of N–H stretch (no peaks in 3340 and 3460 $cm^{-1}$) in the TNPA spectrum, exhibited that it is a tertiary amine. Oppositely, two IR bands at 3340 and 3450 $cm^{-1}$ in the TAPA (reduction product) spectrum were observed which can be attributed to the $–NH_2$ groups,[23] indicating the successful reduction of TNPA to its related amino-compound. Moreover, the peak at 1615.3 $cm^{-1}$ in the TAPA spectrum can be attributed to the N–H bending of primary amines. Besides, the appearance of a peak at 760 $cm^{-1}$ in the reduction product (TAPA) spectrum, related to N–H wang of primary amines, and a shoulder band at 3100 $cm^{-1}$ (primary amines) shines the successful reduction of TNPA to TAPA. The FT–IR spectrum of the as-synthesized TAPA is completely consistented with the previously reported FT–IR for TAPA.[20,24] EDX analysis was carried out to shine the FT–IR results. In this regard, the EDX spectra were recorded for the TNPA (Figure S2a, Supplementary Information) and its reduction product (Figure S6a, Supplementary Information). As shown in Figure S6a (Supplementary Information), after the reduction of TNPA on the surface of AgNPs, the oxygen (O) line was disappeared in the EDX spectrum of the resulted product (TAPA), exhibiting the successful reduction of TNPA over the homogenous AgNPs.

The XRD spectrum of TAPA was also recorded for its characterization (Figure S6b). The XRD peaks positioned at 2θ= 13.239, 24.722, and 29.953 can be assigned to C(110), C(210), and C(310), respectively. Based on the XRD pattern, the d-spacing and the average crystalline size of TAPA were estimated as 4.42 °A and 22.0 nm, respectively. The optical properties of pale-grey-reddish-grey (at 25 °C) TAPA powder were checked by UV–Visible (Figure S7a, Supplementary Information) and FL spectroscopy (Figure S7b, Supplementary Information). Regarding Figure S7a, three absorption peaks at 242 nm, 325 nm, and 405 nm were observed for the TAPA. The peak at 405 nm can be assigned to the triphenylamine part of TAPA.[21] Increasing the $\lambda_{max}$ from 400 nm to 405 nm after the TNPA reduction is related to the electron-donating nature of the $NH_2$ groups of TAPA, as reported.[22] The TNPA shows a peak at 237 nm (related to the nitrophenyl rings), this peak was shifted to 242 nm after the TNPA reduction that is close to the secondary band of the aromatic rings (250 nm)[22,25] due to the electron-donating nature of the $–NH_2$ groups of TAPA, as reported.[22] Based on the above results, it can be concluded that the TNPA was successfully reduced to its corresponding amino-compound, TAPA. Regarding the fluorescence spectrum of TAPA, the excitation and emission wavelengths for the TAPA were observed at 409 nm and 557 nm, respectively.

### 3.4 *Optimization*

Factors affecting the yield of the TNPA reduction in the presence of homogenous AgNPs as H-transfer catalyst and $NaBH_4$ as H-donor, including, temperature, reaction time, mmol of $NaBH_4$, and the catalyst

volume, were optimized (Figure 2a-d). The reduction yield reached its maximum value when 1.0 mmol of $NaBH_4$ (with a final concentration of 8.40 mg $mL^{-1}$) and 4.5 mL of AgNPs (150.0 μg $mL^{-1}$) were used for the heterogeneous reduction of 0.2 mmol of TNPA (with a relative concentration of 16.90 mg $mL^{-1}$) at ambient temperature with a reaction time of 3.0 hours. Based on Figure 2a, the reduction yield was reduced by increasing the reaction temperature, it is maybe due to decreasing the catalytic activity of AgNPs at higher temperatures than 25 °C.[26,27] At optimal conditions, the yield of the TNPA reduction was calculated at about 98.0%.

### 3.5 *Importance of heterogeneous reduction of TNPA*

The importance of the heterogeneous reduction of TNPA was investigated. In this regard, the reduction of TNPA was performed homogeneously with the different volume ratios of EtOH: AgNPs, where EtOH (Merck) was used as a solvent for the TNPA (Figure 3a). Based on Figure 3a, the reduction of TNPA reached its maximum yield when it was heterogeneously reduced on the surface of homogenous AgNPs, however, the reduction yield decreases by increasing the EtOH volume ratio as the solvent of TNPA. At optimal conditions, the reduction process was heterogeneously performed in the presence of AgNPs without using any solvent for TNPA.

### 3.6 *Reusability studies*

Reusability is one of the most important features of a nanocatalyst and points to its cycling stability. Hence, the reusability of the homogenous AgNPs for the reduction of TNPA to its corresponding amino-compound (TAPA) was checked under optimal conditions. To do this, the as-synthesized TAPA was worked up by filtration and crystallization from acetone. After that, the AgNPs contained unreacted $NaBH_4$ were easily collected through the filtration and directly used for the reusability studies, the results showed in Figure 3b. Regarding this figure, the TNPA reduction was successfully performed with a yield of about 98.0% at the first operational time. However, the reduction efficiency was slightly decreased to 92.0%, 85.0%, and 83.0% for the second, third, and fourth reuses, respectively, indicated that the cycling stability of homogenous AgNPs toward TNPA reduction was excellent. Moreover, the reaction yield was found to be high as 72.0% after sixth operational times. It should be mentioned that the $NaBH_4$ (H-donor) is consumed in a stepwise manner in the first and

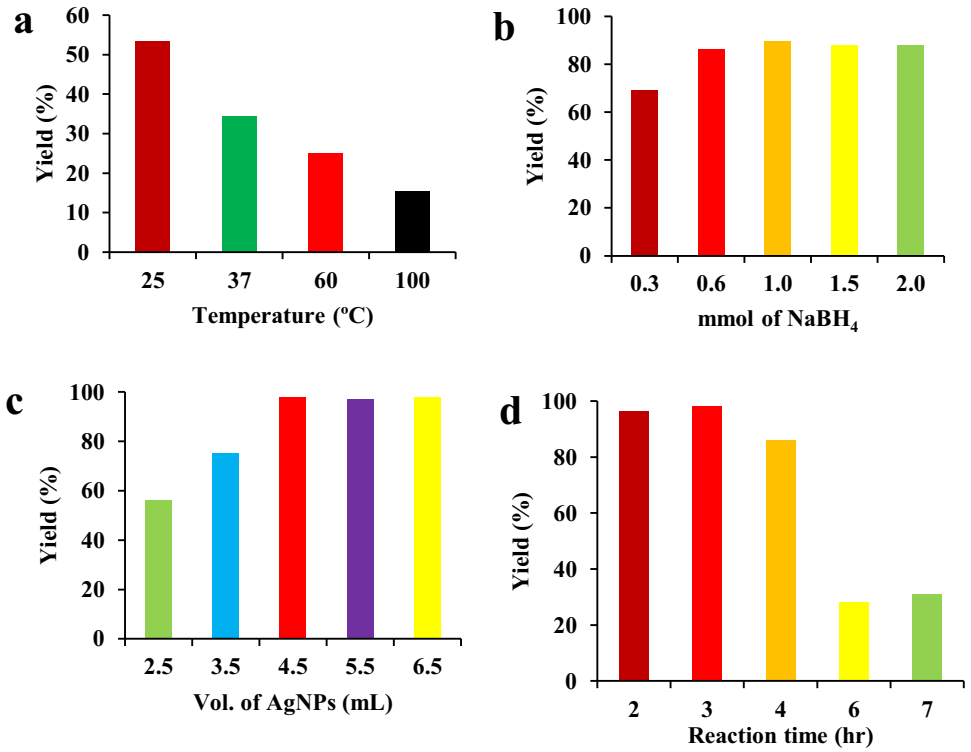


**Figure 2.** Optimization of factors affecting TNPA reduction to TAPA, (a) reaction temperature, (b) mmol of $NaBH_4$, (c) AgNPs volume as H-transfer catalyst, and (d) reaction time.

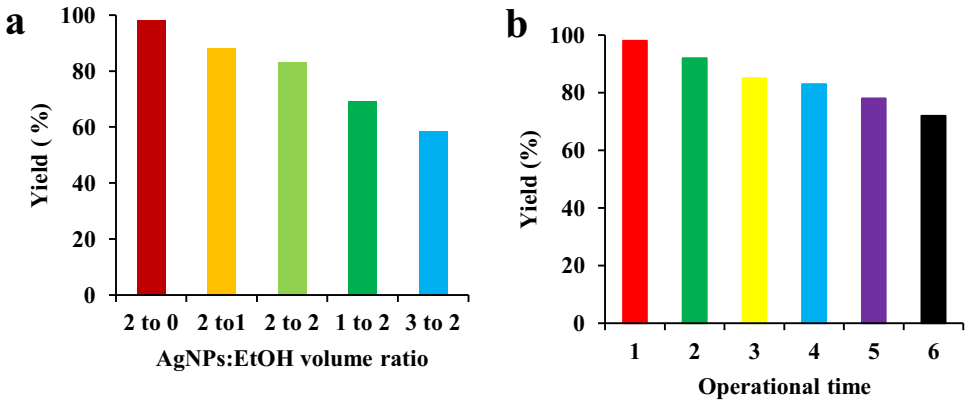


**Figure 3.** Investigation of the importance of the heterogeneous reduction of TNPA (a) and reusability studies (b).

subsequent cycles which affect the reduction yield in the subsequent cycles. On the other hand, the reaction yield was decreased from 98.0% to 72.0% after 6 cycle due to consuming $NaBH_4$ in a stepwise manner. The reusability studies revealed that the AgNPs are high throughput for TNPA reduction with excellent cycling stability. As a consequence, the easy recovery and excellent reusability of homogenous AgNPs along with high reaction yield recommend the great potential of the developed method for application towards the reduction of nitro compounds.

Table S1 (Supplementary Information) shows a typical comparison between the traditional methods of TNPA reduction and the developed method. Regarding this table, the developed method exhibits an improvement in the figures of merits of TNPA reduction than the traditional reduction methods. Besides, the green properties of the developed method for the TNPA reduction were investigated. The proposed catalytic system revealed excellent reusability and high reduction yield as 98.0% with negligible amounts of wastes, proving its green properties. Moreover, the homogenous AgNPs were used as both catalyst and reaction media, and the reduction was performed without using any organic solvent. Hence, it can be concluded that the developed method works through a green chemistry approach which is a significant advantage for the proposed method.

### 3.7 *Proposed mechanism*

The possible mechanism for TNPA reduction to TAPA on the surface of AgNPs was proposed. The interaction between Ag and the nitro group of nitroaromatics was previously studied in the literature.[1,3,6] These studies shined that the Ag(0) of AgNPs was the active form in the catalytic reduction of nitroaromatics. The Ag(0) was oxidized to Ag(I) in the catalytic process by coordination to the nitro groups of the nitro compound, and consequently by activation of nitro-substrate.[3] Based on these considerations, the TNPA reduction to its recommended amino-compound, TAPA, on the surface of homogenous AgNPs as the H-transfer catalyst and in the presence of $NaBH_4$ as the H-donor compound maybe work through a possible Langmuir–Hinshelwood mechanism. The possible mechanism for the TNPA reduction was schematically shown in Scheme 1. The proposed mechanism for the TNPA reduction over the homogenous AgNPs is consistent with the reported mechanism for the reduction of 4-nitrophenol over the textile-supported silver nanoparticles.[3]

## 4. Conclusions

In this contribution, a green, facile, fast, and high throughput reusable catalytic reduction process was developed for the large-scale reduction of tris(p-nitrophenyl)amine to its corresponding amino-compound, tris(p-aminophenyl)amine (TAPA). The homogenous AgNPs and $NaBH_4$ were used as the H-transfer catalyst and the H-donor compound, respectively. The successful reduction of TNPA was investigated by FT–IR, EDX, and XRD analysis, and its optical properties were checked by the UV–Visible and FL spectroscopies. Factors affecting the reduction yield including temperature, reaction time, mmol of $NaBH_4$, and catalyst volume, were optimized. Although the AgNPs are homogenous, both TNPA and TAPA are insoluble in water (AgNPs), hence, the reduction process is heterogeneous. The importance of the heterogeneous reduction of TNPA was investigated, indicated that the reduction yield reached its maximum value when TNPA heterogeneously reduced

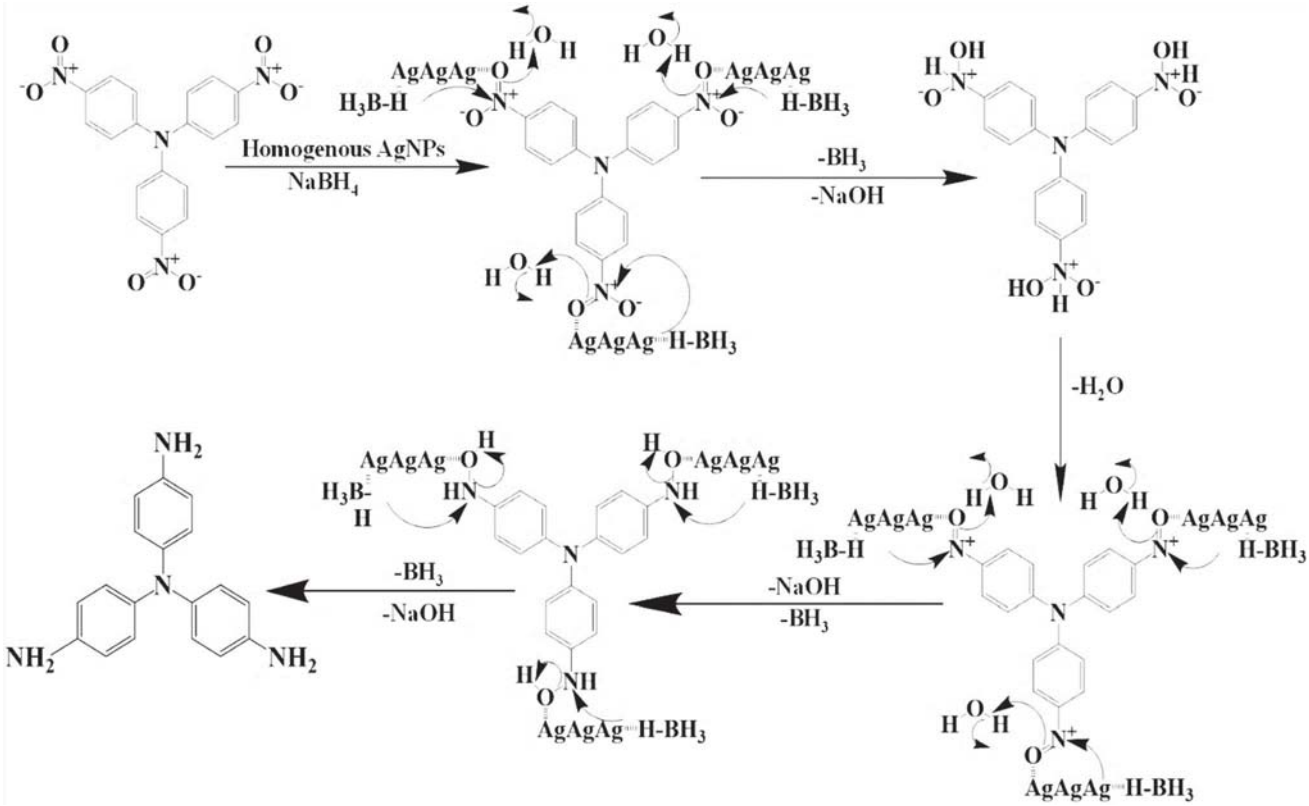


**Scheme 1.** Proposed mechanism for the TNPA reduction to TAPA on the surface of homogenous AgNPs as the H-transfer catalyst.

on the surface of AgNPs. The reduction yield at optimal conditions was calculated at about 98.0% for the first and 72.0% after the 6$^{th}$ operational cycle, respectively. The mechanism of the reduction process was also established, indicated that the process works through a possible Langmuir–Hinshelwood mechanism. The easy recovery and excellent reusability of homogenous AgNPs along with high reaction yield recommend the great potential of the developed method for application towards nitro compounds reduction.

## Supplementary Information (SI)

Figures S1-S7 and Table S1 are available at www.ias.ac.in/chemsci.

## Acknowledgement

The authors wish to acknowledge the support of this work by Shiraz University Research Council.

### Compliance with ethical standards

**Conflicts of interest** The authors declare that they have no known competing for financial interests or personal relationships that could have appeared to influence the work reported in this paper.

## References

1. Gu Y, Jiao Y, Zhou X, Wu A, Buhe B and Fu H 2018 Strongly coupled Ag/$TiO_2$ heterojunctions for effective and stable photothermal catalytic reduction of 4-nitrophenol *Nano Res.* **11** 126
2. Mitsudome T, Mikami Y, Matoba M, Mizugaki T, Jitsukawa K and Kaneda K 2012 Design of a silver–cerium dioxide core-shell nanocomposite catalyst for chemoselective reduction reactions *Angew. Chem. Int. Ed.* **51** 136
3. Feng W, Huang T, Gao L, Yang X, Deng W, Zhou R and Liu H 2018 Textile-supported silver nanoparticles as a highly efficient and recyclable heterogeneous catalyst for nitroaromatic reduction at room temperature *RSC Adv.* **8** 6288
4. Lauwiner M, Roth R and Rys P 1999 Reduction of aromatic nitro compounds with hydrazine hydrate in the presence of an iron oxide/hydroxide catalyst. III. The selective reduction of nitro groups in aromatic azo compounds *Appl. Catal. A: Gen.* **177** 9
5. Gerelbaatar K, Tsogoo A, Dashzeveg R, Tsedev N and Ganbo E 2017 Reduction of 2,4-dinitrophenol to 2,4-

diaminophenol using AuNPs and AgNPs as catalyst *Solid State Phenom.* **271** 76
6. Millán R, Liu L, Boronat M and Corma A 2018 A new molecular pathway allows the chemoselective reduction of nitroaromatics on non-noble metal catalysts *J. Catal.* **364** 19
7. Liu X, Cheng H and Cui P 2014 Catalysis by silver nanoparticles/porous silicon for the reduction of nitroaromatics in the presence of sodium borohydride *Appl. Surf. Sci.* **292** 695
8. Rajesh R and Venkatesan R 2012 Encapsulation of silver nanoparticles into graphite grafted with hyperbranched poly(amidoamine) dendrimer and their catalytic activity towards reduction of nitro aromatics *J. Mol. Catal. A: Chem.* **359** 88
9. Cho A, Byun S and Kim B M 2018 AuPd–$Fe_3O_4$ nanoparticle catalysts for highly selective, one-pot cascade nitro-reduction and reductive amination *Adv. Synth. Catal.* **360** 1253
10. Shokouhimehr M 2015 Magnetically separable and sustainable nanostructured catalysts for heterogeneous reduction of nitroaromatics *Catal.* **5** 534
11. Shokouhimehr M, Hong K, Lee T H, Moon C W, Hong S P, Zhang K, Suh J M, Choi K S, Varma R S and Jang H W 2018 Magnetically retrievable nanocomposite adorned with Pd nanocatalysts: Efficient reduction of nitroaromatics in aqueous media *Green Chem.* **20** 3809
12. Qin L, Yi H, Zeng G, Lai C, Huang D, Xu P, Fu Y, He J, Li B, Zhang C and Cheng M 2019 Hierarchical porous carbon material restricted Au catalyst for highly catalytic reduction of nitroaromatics *J. Hazard. Mater.* **38** 120864
13. Qin L, Huang D, Xu P, Zeng G, Lai C, Fu Y, Yi H, Li B, Zhang C, Cheng M and Zhou C 2019 In-situ deposition of gold nanoparticles onto polydopamine-decorated g-$C_3N_4$ for highly efficient reduction of nitroaromatics in environmental water purification *J. Colloid Interf. Sci.* **534** 357
14. Hu Z, Zhou J, Ai Y, Liu L, Qi L, Jiang R, Bao H, Wang J, Hu J, Sun H B and Liang Q 2018 Two dimensional Rh/$Fe_3O_4$/g-$C_3N_4$-N enabled hydrazine mediated catalytic transfer hydrogenation of nitroaromatics: A predictable catalyst model with adjoining Rh *J. Catal.* **368** 20
15. Krishna Kumar A S, You J G, Tseng W B, Dwivedi G D, Rajesh N, Jiang S J and Tseng W L 2019 Magnetically separable nanospherical g-$C_3N_4$@$Fe_3O_4$ as a recyclable material for chromium adsorption and visible-light-driven catalytic reduction of aromatic nitro compounds *ACS Sustain. Chem. Eng.* **7** 6662
16. Payra S and Banerjee S 2019 Highly efficient and chemoselective reduction of nitroarenes using hybrid Ni@g-$C_3N_4$ as Reusable Catalyst *ChemistrySelect* **4** 9556
17. Zhang K, Suh J M, Choi J W, Jang H W, Shokouhimehr M and Varma R S 2019 Recent advances in the nanocatalyst-assisted $NaBH_4$ reduction of nitroaromatics in Water *ACS Omega* **4** 483
18. Zhang K, Hong K, Suh J M, Lee T H, Kwon O, Shokouhimehr M and Jang H W 2019 Facile synthesis of monodispersed Pd nanocatalysts decorated on graphene oxide for reduction of nitroaromatics in aqueous solution *Res. Chem. Intermed.* **45** 599
19. Li H, Yan X, Qiao S, Lu G and Su X 2018 Yellow-emissive carbon dots based optical sensing platform: cell imaging and analytical applications for biocatalytic reactions *ACS Appl. Mater. Interfaces* **10** 7737
20. El-Mahdy A F, Kuo C H, Alshehri A, Young C, Yamauchi Y, Kim J and Kuo S W 2018 Strategic design of triphenylamine- and triphenyltriazine-based two-dimensional covalent organic frameworks for $CO_2$ uptake and energy storage *J. Mater. Chem. A* **6** 19532
21. Melánová K, Cvejn D, Bureš F, Zima V, Svoboda J, Beneš L, Mikysek T, Pytela O and Knotek P 2014 Organization and intramolecular charge-transfer enhancement in tripodal tris[(pyridine-4-yl)phenyl]amine push–pull molecules by intercalation into layered materials bearing acidic functionalities *Dalton Trans.* **43** 10462
22. Kumar S 2006 Spectroscopy of Organic Compounds, Dept. of Chemistry, Guru Nanak Dev University, pages 14–16.
23. Hormozi Jangi S R, Akhond M and Dehghani Z 2020 High throughput covalent immobilization process for improvement of shelf-life, operational cycles, relative activity in organic media and enzymatic kinetics of urease and its application for urea removal from water samples *Process Biochem.* **90** 102
24. Sun S, Shu Q, Lin P, Li Y, Jin S, Chen X and Wang D 2016 Triphenylamine based lab-on-a-molecule for the highly selective and sensitive detection of $Zn^{2+}$ and $CN^-$ in aqueous solution *RSC Adv.* **6** 93826
25. Buršeš F 2014 Fundamental aspects of property tuning in push–pull molecules *RSC Adv.* **4** 58826
26. Li R S, Liu H, Chen B B, Zhang H Z, Huang C Z and Wang J 2016 Stable gold nanoparticles as a novel peroxidase mimic for colorimetric detection of cysteine *Anal. Methods* **8** 2494
27. Akhond M, Hormozi Jangi S R, Barzegar S and Absalan G 2020 Introducing a nanozyme-based sensor for selective and sensitive detection of mercury (II) using its inhibiting effect on production of an indamine polymer through a stable n-electron irreversible system *Chem. Pap.* **74** 1321